Journal of Green Engineering (JGE)

Volume-10, Issue-12, December 2020

Greens Function Based Analytical Model for Enhanced Defect Detection Using Depth Resolvable Non-Stationary Thermal Wave Imaging

[1]G. V. P. Chandra Sekhar Yadav, [2]V. S. Ghali, [3]B. Sonali Reddy, [4]B. Omprakash, [5]Ch. Chaithanya Reddy

[1,2,3,4,5]Infrared Imaging Center, Department of ECE, Koneru Lakshmaiah Education Foundation, Vaddeswaram, A.P, India. E-mail: [1]sekhar.yadav2008@gmail.com

Abstract

Defect free material characterization without diminishing its future utility has attained the importance and thus, demands a suitable non-destructive testing method. Active infrared thermography becoming a prominent non-destructive testing method to get the depth resolvable subsurface details by imposing a band of low frequencies over the test objects. This work presents a novel analytical model for 3-D heat diffusion equation using greens function based approach to get the temperature response. Further the obtained thermal response has been processed using recently introduced chirp z based post processing modality to get the detail visualization of subsurface details. Later the proposed mathematical model has been experimentally validated by conducting experiment over a carbon fiber reinforced polymer and the results are compared in terms of detection, signal to noise ratio (SNR) and full width at half maxima (FWHM).

Keywords: Active infrared thermography, 3-D heat equation, Greens function, Chirp Z transform and Quadratic frequency modulated thermal wave imaging.

Journal of Green Engineering, Vol. 10_12, 12933-12947.

1 Introduction

During the manufacturing of various industrial materials several defects are produced which reduces their strength, restricts their product applicability, hence a rigorous testing is required prior to their use. Recent past witnessed a tremendous growth in non-destructive testing of these materials for quality assessment and assurance through different approaches. Infrared thermography is one among them which is a full field, remote, fast and non-destructive testing method and assessment is done based on the captured temperature map of the test sample [1-4] to get the surface and subsurface details.

It is possible to divide infrared thermography into passive and active approaches. The passive approach uses the object's natural thermal response to detect anomalies by recognizing the temporal difference between the atmosphere and the testing material. In contrast, a modulated stimulus is used by an active approach to energize the test sample, which is absorbed over the object's surface and produces similar thermal waves within the test sample. The thermal waves propagated inside the object can cause an energy accumulation and generates thermal contrast over the object surface. The surface temperature response is captured using the infrared (IR) camera and further processed using various techniques for extraction of subsurface details.

Pulse and lock-in are the widely used active thermographic approaches to resolve the surface and subsurface details. Requirement of more peak power along with non-uniform heating and radiation limits the use of this approach [2-3]. A number of alternate thermal excitation modalities have been developed for better assessment of results. A continuous modulated heating wave like sinusoidal stimulation is used in lock in thermography, this sinusoidal input excitation generates a periodic thermal wave field inside the object and further corresponding amplitude and phase details of extracted thermal signals are used to visualize the subsurface anomalies [4]. But this mono frequency sinusoidal stimulus limits the maximum detection capability and furthermore it is time consuming. In order to overcome this limitation, linear frequency modulated chirped stimulus of low power was introduced to probe a band of low frequencies [5] in a single experimentation cycle over the surface of the test object to get the depth resolved details underneath the test specimen. Later quadratic frequency modulated chirped stimulus with low peak power was used to probe over the experimental side of the object as the quadratic version of chirped stimulus probes more deep into the object at low frequencies than its linear counterpart [6], thus reveals the subsurface details with better contrast. Since the probing of band of frequencies scans anomalies with different sizes located at different depths with fine resolution and also avoids the concept of blind frequencies in processing time.

The recorded thermal response is processed using multiple processing algorithms like fast fourier transform, matched filter based correlation (pulse

compression), Hilbert transform, random projection transform and chirpz transform. To assess the proposed modality, the experimentation is conducted on carbon fiber reinforced polymer (CFRP). Further obtained results are compared with the conventional post processing approaches by considering the SNR and FWHM as performance evaluation metrics.

2 Literature Survey

Several studies were performed to get the temperature response of 1-D and 3-D heat diffusion equation for single layer and multi-layer structures [5-15] in non-stationary thermography. R. Mulaveesala [5], introduced frequency modulated (FM) thermal wave imaging and validated the analytical model experimentally on CFRP specimen of Teflon patches using pulse compression based modality. Later V.S. Ghali [6], proposed a mathematical model for 1-D heat equation using quadratic frequency modulated (QFM) chirp input and validated it for GFRP of Teflon patches. Later, in 2017 & 2018 V. S. Ghali and his team [7-8] come up with a quantitative analytical model ever first in non-stationary thermography for 1-D heat diffusion equation using FM and QFM chirp inputs and validated the phase based depth experimentally for CFRP and mild steel of artificially made flat bottom holes using chirp Z transform based post processing modality. A continuous research has been progressing from his team members Sk. Subhani et.al, to assess the thermal diffusivity of the experimental CFRP specimen [9] using the 1-D heat diffusion equation and proposed a classification and regression based quantitative analytical model by considering back wave reflection from the defect [10].

Recently, A. Vijaya Lakshmi, [11] presented an automatic classification and regression tree based quantification for quadratic frequency modulated chirp excitation by solving 1-D heat equation for multi-layer structure. Further, R. Mulaveesala [12], developed an analytical model for surface temperature response by using 3-D heat diffusion equation for single and multi-layer structures.

3 Proposed Methodology

The present work uses various signal processing techniques to elevate the fine subsurface details. In general defects may be generated at various locations; in order to discriminate the closely separated defects a depth resolution based post processing modality is required. As frequency resolution is directly proportional to depth resolution as given by eq.1. If ∂f is small, then it reduces $\partial \mu$, which leads to more depth resolution. ∂f is reduces by zooming a specific band of low frequencies which is possible with the recently proposed chirp Z transform [7-8] unlike conventional FFT based phase approach. FFT based phase approach gives the limited frequency resolution by zooming entire band, whereas CZT based approach zooms a

specific band of low frequencies (0.01-0.02Hz) for m (8192) number of samples that leads to small ∂f which increases the frequency resolution there by increases the depth resolution.

$$\partial\mu\alpha\left|\sqrt{\frac{\alpha}{\pi}}\left(f^{-3/2}\right)\right|\partial f \tag{1}$$

4 Mathematical Modeling

The temperature response on the surface of the material has been obtained by solving the 3-D heat equation by considering internal heat generation Q_m. The mathematical model is obtained by using Greens function under the Neumann boundary conditions [12].

Consider 3-D diffusion equation

$$\frac{\partial^2 T(x,y,z,t)}{\partial^2 x}+\frac{\partial^2 T(x,y,z,t)}{\partial^2 y}+\frac{\partial^2 T(x,y,z,t)}{\partial^2 z}=\frac{1}{\alpha}\frac{\partial T(x,y,z,t)}{\partial t}+Q_m \tag{2}$$

Where α refers the thermal diffusivity of the test specimen. The solution is acquired by resolving the homogeneous section of eq.2 using variable separable method and it can be written as

$$T(x,y,z,t)=X(x)Y(y)Z(z)\Gamma(t) \tag{3}$$

By substituting eq.3 in eq.2

$$\frac{\partial^2(X(x)Y(y)Z(z)\Gamma(t))}{\partial^2 x}+\frac{\partial^2(X(x)Y(y)Z(z)\Gamma(t))}{\partial^2 y}+\frac{\partial^2(X(x)Y(y)Z(z)\Gamma(t))}{\partial^2 z}=\frac{1}{\alpha}\frac{\partial X(x)Y(y)Z(z)\Gamma(t))}{\partial t} \tag{4}$$

$$\frac{Y(y)Z(z)\Gamma(t)\partial^2 X(x)}{\partial^2 x}+\frac{X(x)Z(z)\Gamma(t)\partial^2 Y(y)}{\partial^2 y}+\frac{X(x)Y(y)\Gamma(t)\partial^2 Z(z)}{\partial^2 z}=\frac{1}{\alpha}\frac{X(x)Y(y)Z(z)\partial\Gamma(t)}{\partial t} \tag{5}$$

Divide with $X(x)Y(y)Z(z)\Gamma(t)$ on both sides

$$\frac{X^{"}(x)}{X(x)}+\frac{Y^{"}(y)}{Y(y)}+\frac{Z^{"}(z)}{Z(z)}=\frac{1}{\alpha}\frac{\Gamma^{"}(t)}{\Gamma(t)} \tag{6}$$

Let $$\frac{X^{"}(x)}{X(x)}=-\beta^2;\frac{Y^{"}(y)}{Y(y)}=-\gamma^2;\frac{Z^{"}(z)}{Z(z)}=-\eta^2;\frac{\Gamma^{"}(t)}{\Gamma(t)}=-\lambda^2 \tag{7}$$

Put eq.7 in eq. 6, we get $-\beta^2-\gamma^2-\eta^2=-\frac{\lambda^2}{\alpha}$

$$\lambda^2=\alpha(\beta^2+\gamma^2+\eta^2) \tag{8}$$

Since the solutions are negative

$$\begin{aligned} X(x) &= A_1 \cos \beta x + B_1 \sin \beta x \\ Y(y) &= A_2 \cos \gamma y + B_2 \sin \gamma y \\ Z(z) &= A_3 \cos \eta z + B_3 \sin \eta z \\ \Gamma(t) &= Ce^{-\alpha(\beta^2+\gamma^2+\eta^2)t} \end{aligned} \tag{9}$$

Substitute eq.9 in eq.3

$$T(x,y,z,t) = (A_1 \cos \beta x + B_1 \sin \beta x)(A_2 \cos \gamma y + B_2 \sin \gamma y)(A_3 \cos \eta z + B_3 \sin \eta z)Ce^{-\alpha(\beta^2+\gamma^2+\eta^2)t} \tag{10}$$

Boundary conditions and initial conditions are

$$\begin{aligned} &-k\frac{\partial T}{\partial x}\Big|_{x=0} = Q_T(t); -k\frac{\partial T}{\partial x}\Big|_{x=a} = 0; \\ &-k\frac{\partial T}{\partial y}\Big|_{y=0,b} = 0; \\ &-k\frac{\partial T}{\partial z}\Big|_{z=0,c} = 0; \\ &T(x,y,z,0) = T_0; \end{aligned} \tag{11}$$

Where $Q_T(t)$ is the combination of DC and QFM chirp signal i.e., $Q_T(t)=1+Q(t)$

Q(t) is the QFM chirp signal; 1 is the DC added to QFM to overcome the simultaneous heating and cooling phase of experimentation $Q_T(t) = Q_0\left(1+e^{j2\pi(f_0+b_0t^2)t}\right); x=0$. Where, Q_0 refers constant heat flow, f_0 refers starting frequency and b_0 refers the chirp rate of the incident QFM chirp signal. Fig.1 represents the DC added QFM chirp signal of 2kw power at 0.01-0.1Hz frequency.

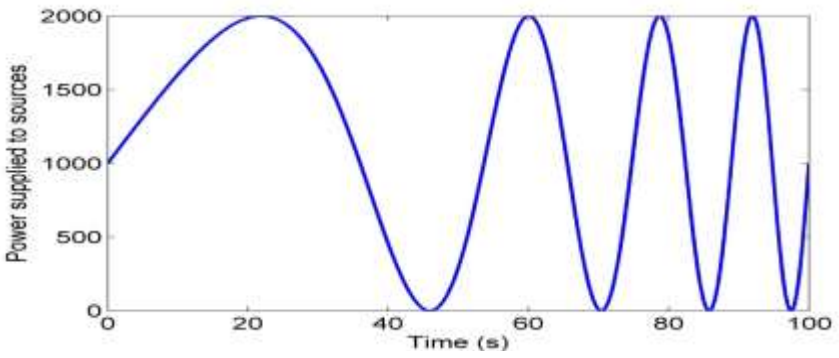

Figure 1 Incident Quadratic Frequency Modulated Chirped Signal with 0.01-0.1Hz Frequency

By substituting eq.11 in eq.10, we get solution for Greens function for eq.2 [12]

$$G(x,y,z,t;\varepsilon,\xi,\delta,\tau)=\frac{R_1R_2R_3}{abc}\sum_{m=0}^{\infty}\sum_{n=0}^{\infty}\sum_{p=0}^{\infty}\cos\beta_m x\cos\beta_m\varepsilon\cos\gamma_n y\cos\gamma_n\xi\cos\eta_p z\cos\eta_p\delta e^{-\alpha(\beta_m^2+\gamma_n^2+\eta_p^2)(t-\tau)} \tag{12}$$

Where

$$\beta_m=\frac{m\pi}{a};\ m=0,1,2....\infty$$
$$\gamma_n=\frac{n\pi}{b};\ n=0,1,2....\infty$$
$$\eta_p=\frac{p\pi}{c};\ p=0,1,2....\infty$$
$$R_1=\begin{cases}1;\ m=0\\ 2;\ m=1,2....\infty\end{cases}$$
$$R_2=\begin{cases}1;\ n=0\\ 2;\ n=1,2....\infty\end{cases}$$
$$R_3=\begin{cases}1;\ p=0\\ 2;\ p=1,2....\infty\end{cases}$$

In terms of Greens function the solution for eq.2 which refers non-homogeneous heat diffusion is given as

$$\begin{aligned}T(x,y,z,t)=&\frac{\alpha}{k}\int_0^t\int_0^a\int_0^b\int_0^c Q_m G(x,y,z,t;\varepsilon,\xi,\delta,\tau)d\delta d\xi d\varepsilon d\tau\\ &-\alpha\int_0^t\int_0^b\int_0^c T(\varepsilon,\xi,\delta,\tau)\nabla_j G(x,y,z,t;\varepsilon,\xi,\delta,\tau)d\delta d\xi d\tau\\ &+\alpha\int_0^t\int_0^b\int_0^c G(x,y,z,t;\varepsilon,\xi,\delta,\tau)\nabla_j T(\varepsilon,\xi,\delta,\tau)d\delta d\xi d\tau\\ &+\int_0^a\int_0^b\int_0^c T(\varepsilon,\xi,\delta,0)G(x,y,z,t;\varepsilon,\xi,\delta,0)d\delta d\xi d\varepsilon\end{aligned} \tag{13}$$

$$\begin{aligned}T(x,y,z,t)=&\frac{\alpha}{k}\int_0^t\int_0^a\int_0^b\int_0^c Q_m G(x,y,z,t;\varepsilon,\xi,\delta,\tau)d\delta d\xi d\varepsilon d\tau\\ &+\alpha\int_0^t\int_0^b\int_0^c G(x,y,z,t;0,\xi,\delta,\tau)\frac{\partial T(0,\xi,\delta,\tau)}{\partial x}d\delta d\xi d\tau\\ &-\alpha\int_0^t\int_0^b\int_0^c G(x,y,z,t;a,\xi,\delta,\tau)\frac{\partial T(a,\xi,\delta,\tau)}{\partial x}d\delta d\xi d\tau\\ &+\int_0^a\int_0^b\int_0^c T(\varepsilon,\xi,\delta,0)G(x,y,z,t;\varepsilon,\xi,\delta,0)d\delta d\xi d\varepsilon\end{aligned} \tag{14}$$

Apply the boundary conditions and initial conditions from eq.11 to above eq.14, we get

$$T(x,y,z,t) = \begin{aligned} &\frac{\alpha}{k}\int_0^t\int_0^a\int_0^b\int_0^c Q_m G(x,y,z,t;\varepsilon,\xi,\delta,\tau)\,d\delta\,d\xi\,d\varepsilon\,d\tau \\ &-\frac{\alpha}{k}\int_0^t\int_0^b\int_0^c G(x,y,z,t;0,\xi,\delta,\tau)Q_T(\tau)\,d\delta\,d\xi\,d\tau \\ &+\int_0^a\int_0^b\int_0^c T(\varepsilon,\xi,\delta,0)G(x,y,z,t;\varepsilon,\xi,\delta,0)\,d\delta\,d\xi\,d\varepsilon \end{aligned} \quad (15)$$

In the case of experimentation $Q_T(t)$ is considered as the combination of DC and QFM chirp signal to overcome the simultaneous heating and cooling process.

After the experimentation while doing the qualitative analysis, DC response was removed as it doesn't contain any information.

Hence the final temperature equation can be obtained from eq.15 is

$$T(x,y,z,t) = -\frac{\alpha}{k}\int_0^t\int_0^b\int_0^c G(x,y,z,t;0,\xi,\delta,\tau)Q(\tau)\,d\delta\,d\xi\,d\tau \quad (16)$$

By substituting Greens function from eq.12 the above eq.16 can be written as

$$T(x,y,z,t) = -\frac{\alpha}{k}\int_0^t\int_0^b\int_0^c \frac{R_1R_2R_3}{abc}\sum_{m=0}^{\infty}\sum_{n=0}^{\infty}\sum_{p=0}^{\infty}\cos\beta_m x\cos\gamma_n y\cos\gamma_n\xi\cos\eta_p z\cos\eta_p\delta e^{-\alpha(\beta_m^2+\gamma_n^2+\eta_p^2)(t-\tau)}Q(\tau)\,d\delta\,d\xi\,d\tau \quad (17)$$

$$T(x,y,z,t) = -\frac{\alpha}{k}\int_0^t \frac{R_1}{a}\sum_{m=0}^{\infty}\cos\beta_m x e^{-\alpha(\beta_m^2)(t-\tau)}Q(\tau)\,d\tau \quad (18)$$

$$T(x,y,z,t) = -\frac{\alpha}{ka}\int_0^t\left(1+2\sum_{m=1}^{\infty}\cos\beta_m x e^{-\alpha(\beta_m^2)(t-\tau)}\right)Q(\tau)\,d\tau \quad (19)$$

By considering m=0 and 1 and neglecting higher order m values because

$$\cos\beta_m x = 1; m = 0,1,2,3....\infty \text{ for } a = 0.005m$$

$$e^{-\alpha(\beta_m^2)(t-\tau)} = e^{-0.42*10^{-6}\left(\frac{m\pi^2}{25*10^{-6}}\right)(t-\tau)} \begin{aligned} &=1 && ;m=0\\ &=0.84 && ;m=1\\ &=0.515 && ;m=2\\ &=0.22 && ;m=3\\ &=0.07 && ;m=4\\ &=0.015 && ;m=5\\ &=0.002 && ;m=6\\ &=0.0002 && ;m=7\\ &=0.00002 && ;m=8 \end{aligned}$$

On the application of Laplace transform, we get

$$T(X,Y,Z,s) = -\frac{\alpha}{ka}\frac{Q(s)}{s} + \frac{2\alpha\cos\beta_m x}{ka}\int_0^t\left(\sum_{m=1}^{\infty} e^{-\alpha(\beta_m^2)(t-\tau)}\right)Q(\tau)d\tau$$

$$T(X,Y,Z,s) = -\frac{\alpha}{ka}\frac{Q(s)}{s} + \frac{2\alpha\cos\left(\frac{\pi}{a}x\right)}{ka}\int_0^t e^{-\frac{\alpha(\pi^2)(t-\tau)}{a^2}}Q(\tau)d\tau$$

$$T(X,Y,Z,s) = -\frac{\alpha}{ka}\frac{Q(s)}{s} + \frac{2\alpha\cos\left(\frac{\pi}{a}x\right)}{ka}\frac{e^{-\frac{\alpha\pi^2 t}{a^2}}Q\left(s-\frac{\alpha\pi^2}{a^2}\right)}{s} \quad (20)$$

Where Q(s) refers the Laplace transform of Q(t) at x=0, α is thermal diffusivity of the test sample, k refers the thermal conductivity of the material and a is the length in x-direction respectively. Further, the obtained thermal response is analyzed by different processing algorithms to get the detail visualization.

5 Results and Discussions

Optical excitation provided to the surface of an object breaks the thermal equilibrium and generates thermal contrast over the surface which propagates into subsurface layers as heat waves. Thermography analyses the variations in the thermal contrast created over either of the surfaces due to the reflection of thermal waves from defects at subsurface layers or surface non-uniformity using a thermal camera. The present article uses a quadratic frequency chirp signal with a band of low frequencies [13]. Fig.2.a shows the schematic of experimental set up of quadratic frequency modulated thermal wave imaging, with the aid of paired heat sources each of 1kW, a quadratic frequency modulated chirp signal of 0.01-0.1 Hz frequency is imposed on the experimental side of the specimen and the response obtained from the specimen is recorded simultaneously using the IR camera placed 1m distance from the object, the entire process is controlled by using a control unit. The proposed model is validated by conducting experimentation on the CFRP specimen of size 24x24x0.5cm with 36 artificially created circular holes of various sizes at various depths shown in fig.2.b.

In order to facilitate qualitative and quantitative analysis, a pixel value from all the frames of recorded thermal response is extracted and constitute it as a thermal profile which is analogous to the input stimulus with both static and dynamic responses [14]. Since Static response doesn't give any quantitative information, it is removed by using suitable fitting algorithm and the leftover dynamic response is then analysed by employing various signal processing tools to get qualitative and quantitative surface and subsurface characteristics.

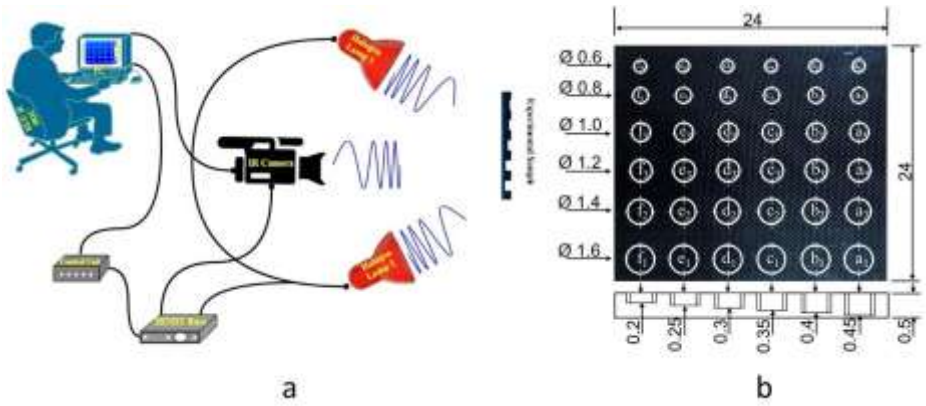

Figure 2(a) Schematic of experimental set-up (**b)** Layout of experimental CFRP

FFT is employed in phase analysis on the dynamic thermal data and each pixel's extracted phase response is arranged in the appropriate positions to get the phasegrams as given by eq. 21. The phase contrast obtained from a particular phasegram is used to discriminate the defective and non-defective locations.

$$Y(K) = \sum_{k=1}^{N} y(n) e^{\left(\frac{-j2\pi nK}{N}\right)} \tag{21}$$

In Hilbert transform, a pixel profile is chosen as a reference thermal profile and this reference profile is processed through Hilbert transform and this resultant profile is cross correlated with each thermal profile as given by the following eq.22.

$$C_1 = IFFT\left\{\{FFT\left(Hilb(Y_r)\right)\}*\{FFT(Y)\}\right\} \tag{22}$$

Correspondingly, the chosen reference thermal profile is cross correlated with each thermal profile by using eq.23 and the phase is extracted using eq.24

$$C_2 = IFFT\left\{\{FFT\left(Y_r\right)\}*\{FFT(Y)\}\right\} \tag{23}$$

$$\phi_{HP} = \tan^{-1}\left(\frac{C_1}{C_2}\right) \tag{24}$$

The phase contrast obtained from the Hilbert phasegram is used to characterize the defective locations [17].

In correlation based matched filter approach, a pixel profile from substrate is considered as a reference profile and this reference profile is correlated with all the pixel profiles and arranged in respective positions corresponding to their peak delay [18-19] to construct the correlation image as given by eq.25. The normalized correlation contrast form a correlation image discriminates the coatings of thin layers.

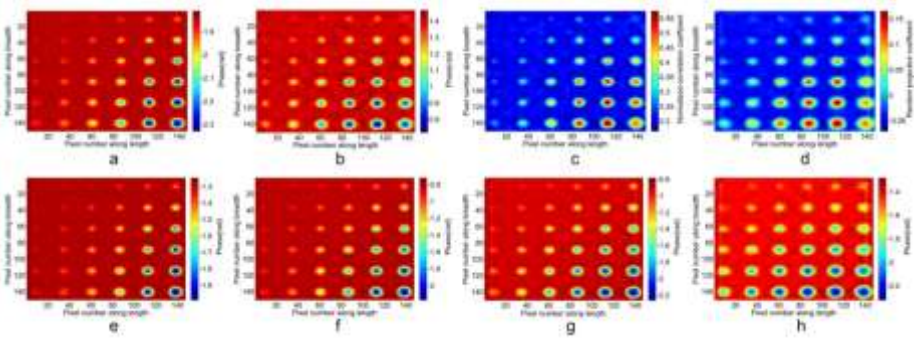

Figure 3 Processed results of CFRP sample for QFMTWI (**a)** FFT phase at 0.05Hz (**b)** Hilbert phase at 14.65s (**c)** Correlation image at 7.8s (**d)** Random projection image at 4th component (**e-h)** CZT phase images at 0.01183Hz, 0.01113Hz, 0.01066Hz and 0.01023Hz respectively

$$g(\tau) = \int_{-\infty}^{+\infty} s(t)h(\tau+t)dt \tag{25}$$

Orthonormal projection transform is a powerful dimensionality reduction method; the algorithm used in this technique is Gram Schmidt. In this method dimensionality reduction can be done by linear transformation of original data from original vector space to a lower dimensional subspace [20]. In this method the original 3-D captured thermal response is transformed into 2-D data by arranging spatial differences occurred in column order and thermal differences occurred in row order and mean value across each row of the matrix is subtracted. An orthonormal set is generated using Gram Schmidt method from the converted two dimensional matrixes. Further the original data is projected on derived basis vectors which give random projection component along column wise [21]. Finally the desired thermal contrast component is chosen from set of components.

$$V_1 = \frac{f_1[n]}{|f_1[n]|}; V_2 = f_2[n] - \left(V_1{}^T f_2[n]\right)V_1 \tag{26}$$

In CZT based post processing technique, a particular band of frequencies are selected from FFT based phase approach and zoomed for 'm' number of frames to get the detailed defect defection with fine depth resolution through frequency resolution [7-8].

Results of CZT based phase analysis are compared with conventional FFT phase, Hilbert phase, matched filter based correlation approach and orthonormal projection transform as shown in fig 3. From the results, it is clear that CZT based phase analysis clearly discriminates the defects of axially closely separated than the conventional techniques.

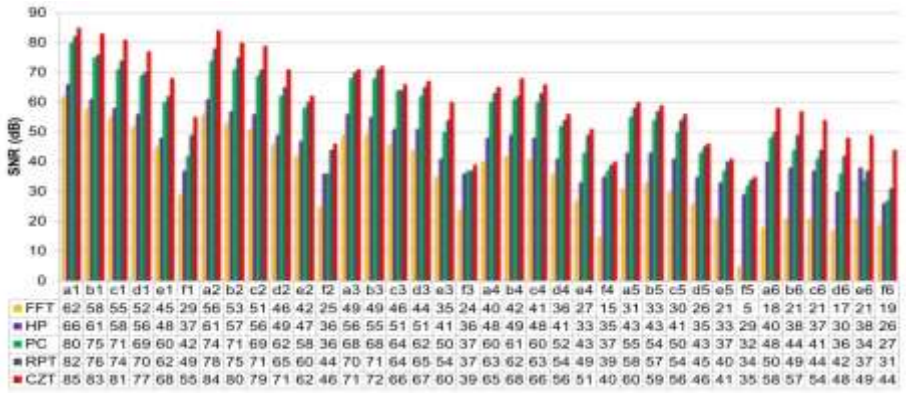

Figure 4 Comparison of SNR of defects for processed results of FFT, HP, PC, RPT and CZT

Defect detectability of the processing method is explained by calculating the SNR of each defect by using the mean of defective, non-defective regions and standard deviation of the non-defective region [22-23] using eq.27

$$SNR = 20\log\left(\frac{mean\ of\ defective\ area - mean\ of\ non\ defecive\ area}{standard\ deviation\ of\ non\ defective\ area}\right) \quad (27)$$

From fig.4, it shows that CZT based post-processing approach detects the defects better than conventional post processing techniques by means of SNR.

The qualitative subsurface analysis is done by estimating the size of defects. A widely used thermographic performance metric [24] FWHM is estimated and its respective defect diameters are shown in the following tabe1. Table1 compares the actual diameter of the defects with estimated FWHM for processed results and its corresponding error value. CZT based post-processing approach gives the nearest diameters of the defects than the conventional techniques.

Table1 Comparison of FWHM of defects of last column for processed results of FFT phase, HP, PC, RPT and CZT phase

Defect	**Actual defect size (in cm)**	**Estimated size (in cm)**									
		FFT phase	***% of Error***	***HP***	***% of Error***	***PC***	***% of Error***	***RPT***	***% of Error***	***CZT phase***	***% of Error***
a_1	1.6	1.47	8.84	1.48	8.11	1.48	8.11	1.605	0.31	1.601	0.06
a_2	1.4	1.45	3.45	1.45	3.45	1.43	2.10	1.41	0.71	1.405	0.36
a_3	1.2	1.09	10.09	1.12	7.14	1.14	5.26	1.195	0.42	1.203	0.25
a_4	1.0	0.95	5.26	0.97	3.09	0.96	4.17	1.01	0.99	1.01	0.99
a_5	0.8	0.71	12.68	0.7	14.29	0.73	9.59	0.805	0.62	0.804	0.50
a_6	0.6	0.46	30.43	0.55	9.09	0.51	17.65	0.59	1.69	0.601	0.17

6 Conclusion

The present work introduces a novel analytical model implemented for a 3-D heat diffusion equation with the aid of greens function to elevate subsurface characteristics. Chirpz transform based processing technique is implemented to reveal the axially closely separated defects with the support of depth resolution through frequency resolution. The proposed technique is validated by conducting experiment over the carbon fiber reinforced polymer of artificially made flat bottom holes of various diameters of various depths and comparing the processed results by means of detection, SNR and FWHM Phase based quantification has to be done as a future work by extracting the phase value from the analytical model supported by 3-D heat diffusion equation with the aid of greens function and validated by comparing with the experimental phase value.

Acknowledgements

This work was supported by Naval Research Board, DRDO and India under the grant no. NRB-423/MAT/18-19 and also partially supported by FIST sponsored ECE Department under the grant no. SR/FST/ET-II/2019/450.

References

[1] X. P. V. Maldague. “Theory and Practice of Infrared Thermography for Non-destructive Testing”, New York Wiley, 2001.

[2]D. Benítez Hernán. “Definition of a New Thermal Contrast and Pulse Correction for Defect Quantification in Pulsed Thermography”, Infrared Physics & Technology, Vol. 51, no. 3, pp. 160–167, 2008.

[3]C. I. Castanedo, N. P. Avdelidis, and X. P. V. Maldague. “Quantitative Pulsed Phase Thermography Applied to Steel Plates”, Proceedings, Thermosense XXVII, Vol. 5782, 2005.

[4]A. Castelo, A. Mendioroz, R. Celorrio, and A. Salazar. “Optimizing the Inversion Protocol to Determine the Geometry of Vertical Cracks from Lock-in Vibrothermography”, Journal of Nondestructive Evaluation, Vol. 36, no. 1, 2016.

[5]R. Mulaveesala and S. Tuli. “Theory of Frequency Modulated Thermal Wave Imaging for Nondestructive Subsurface Defect Detection", Applied Physics Letters, Vol. 89, no. 19, 2006.

[6]Subbarao, Ghali Venkata, and Ravibabu Mulaveesala. “Quadratic Frequency Modulated Thermal Wave Imaging For Non-Destructive Testing”, Progress In Electromagnetics Research , Vol. 26, pp. 11-22, 2012.

[7]B. Suresh, Sk. Subhani, A. Vijaya Lakshmi, V. H. Vardhan and VS Ghali. “Chirp Z Transform Based Enhanced Frequency Resolution for

Depth Resolvable Non Stationary Thermal Wave Imaging", Review of Scientific Instruments, Vol. 88, no. 1, 2017.

[8]Sk. Subhani, B. Suresh and V. S. Ghali. "Quantitative Subsurface Analysis Using Frequency Modulated Thermal Wave Imaging", Infrared Physics & Technology, Vol. 88, pp. 41–47, 2018.

[9]Subhani, Sk., and V.s. Ghali. "Measurement of Thermal Diffusivity of Fiber Reinforced Polymers Using Quadratic Frequency Modulated Thermal Wave Imaging", Infrared Physics & Technology, Vol. 99, pp. 187–192, 2019.

[10]A. Vijaya Lakshmi, V. Gopi Tilak, M. M. Parvez, Sk. Subhani and V. S. Ghali. "Artificial Neural Networks Based Quantitative Evaluation of Subsurface Anomalies in Quadratic Frequency Modulated Thermal Wave Imaging", Infrared Physics & Technology, Vol. 97, pp. 108–115, 2019.

[11]A. Vijaya Lakshmi, V. S. Ghali and Sk. Subhani. "Automated Quantitative Subsurface Evaluation of Fiber Reinforced Polymers", Infrared Physics & Technology, Vol. 110, 2020.

[12]Anshul Sharma, Ravibabu Mulaveesala and Vanita Arora. "Novel Analytical Approach for Estimation of Thermal Diffusivity and Effusivity for Detection of Osteoporosis", IEEE Sensors, Vol. 20, no.11, pp. 6046-6054, 2020.

[13]Sk. Subhani, B. Suresh and V. S. Ghali. "Empirical Mode Decomposition Approach for Defect Detection in Non-Stationary Thermal Wave Imaging", NDT & E International, vol. 81, pp. 39–45, 2016.

[14]M. M. Parvez, J. Shanmugam and V. S. Ghali. "Decision Tree-Based Subsurface Analysis Using Barker Coded Thermal Wave Imaging", Infrared Physics & Technology, vol. 109, 2020.

[15]M. M. Pasha, B. Suresh, K. R. Babu, Sk. Subhani and G. V. Subbarao. "Barker coded modulated thermal wave imaging for defect detection of glass fiber reinforced plastic", ARPN Journal of Engineering and Applied Sciences, Vol. 13, no. 10, pp. 3475- 3480, 2018.

[16]Sk. Subhani, B. Suresh, K. R. Babu, K. S. Lakshmi and G. V. Subbarao. "Recent advances in subsurface analysis with quadratic frequency modulated thermal wave imaging", Journal of Theoretical and Applied Information Technology, Vol. 95, no. 9, pp. 2046-2053, 2017.

[17]M. M. Pasha, G. V. Subbarao, B. Suresh and S. Tabassum. "Inspection of Defects in CFRP Based on Principal Components", International Journal of Recent Technology and Engineering Regular Issue, Vol. 8, no. 3, pp. 2367–2370, 2019.

[18]Sk. Subhani, G. V. P. Chandra Sekhar Yadav and V. S. Ghali. "Defect Characterisation Using Pulse Compression-Based Quadratic Frequency Modulated Thermal Wave Imaging", IET Science, Measurement & Technology, Vol. 14, no. 2, pp. 165–172, 2020.

[19]B. Suresh. "Advanced Signal Processing Approaches for Quadratic Frequency Modulated Thermal Wave Imaging", International Journal of Emerging Trends in Engineering Research, Vol. 7, no. 11, pp. 599–603, 2019.

[20]B. Suresh, Sk. Subhani, V. S. Ghali and R. Mulaveesala. "Subsurface Detail Fusion for Anomaly Detection in Non-Stationary Thermal Wave Imaging", Insight - Non-Destructive Testing and Condition Monitoring, Vol. 59, no. 10, pp. 553–558, 2017.

[21]Sk. Subhani, B. Suresh and V. S. Ghali. "Orthonormal Projection Approach for Depth-Resolvable Subsurface Analysis in Non-Stationary Thermal Wave Imaging", Insight - Non-Destructive Testing and Condition Monitoring, Vol. 58, no. 1, pp. 42–45, 2016.

[22]B. Suresh, J. Sai Kiran and G. V. Subbarao. "Automatic detection of subsurface anomalies using non-linear chirped thermography", International Journal of Innovative Technology and Exploring Engineering, Vol. 8, no. 6, pp. 1247-1249, 2019.

[23]A. Vijaya Lakshmi, V. S. Ghali, M. M. Parvez, G. V. P. Chandra Sekhar Yadav and V. Gopi Tilak. "Fuzzy C-Means Clustering Based Anomalies Detection in Quadratic Frequency Modulated Thermal Wave Imaging", International Journal of Recent Technology and Engineering Regular Issue, Vol. 8, no. 3, pp. 4047–4051, 2019.

[24]A. Vijaya Lakshmi. "A Machine Learning Based Approach for Defect Detection and Characterization in Non-Linear Frequency Modulated Thermal Wave Imaging", International Journal of Emerging Trends in Engineering Research, Vol. 7, no. 11, pp. 517–522, 2019.

Biographies

G.V.P Chandra Sekhar Yadav received his B. Tech degree in Electronics and Communication Engineering from JNTU Kakinada in 2012, M. Tech degree in Digital Electronics & Communication Systems from JNTU Kakinada in 2015 and his area of interest includes Infrared Thermography, Non Destructive Testing & Evaluation, Thermal wave Imaging and Signal processing. Presently he is working as a Research scholar at Infrared Imaging Center, Department of Electronics and Communication Engineering, KLEF, Vaddeswaram, Andhra Pradesh, India.

V.S. Ghali received his M. Sc degree in Electronics from Acharya Nagarjuna University, Guntur, India, in 1998 and the M.E degree in Applied Electronics from Satyabama University, Chennai, India in 2008. He received his Ph. D degree from IIITDM, Jabalpur India in 2013. He is a recipient of research award from University grant commission, India in 2014. Currently he belonged to Infrared Imaging Center and also Professor in ECE, College of Engineering, K L E F, Vaddeswaram, Andhra Pradesh, India. His research interest include Infrared non-destructive testing, Biomedical image processing, Image processing, Signal processing, Machine learning and artificial intelligence.

B. Sonali Reddy is pursuing her B. Tech degree in E C E at K L E F, Vaddeswaram, Andhra Pradesh, India.

B. Omprakash is pursuing his B. Tech degree in E C E at K L E F, Vaddeswaram, Andhra Pradesh, India.

Ch. Chaithanya Reddy is pursuing his B. Tech degree in E C E at K L E F, Vaddeswaram, Andhra Pradesh, India.